Available online at www.sciencedirect.com

ScienceDirect

Ceramics International 40 (2014) 1693–1698

CERAMICS INTERNATIONAL

www.elsevier.com/locate/ceramint

Electrodeposition for the synthesis of ZnO nanorods modified by surface attachment with ZnO nanoparticles and their dye-sensitized solar cell applications

Yongming Meng, Yu Lin*, Yibing Lin

College of Material Science and Engineering, Engineering Research Center of Environment-Friendly Functional Materials for Ministry of Education, Huaqiao University, Xiamen, Fujian 361021, People's Republic of China

Received 16 June 2013; received in revised form 13 July 2013; accepted 13 July 2013
Available online 21 July 2013

Abstract

This paper reports a two-step electrochemical deposited route for the synthesis of ZnO nanorods modified by surface attachment with ZnO nanoparticles and their dye-sensitized solar cell applications. X-ray powder diffraction and a field emission scanning electron microscope were used to investigate the effects of the electrodeposited parameters on the crystal phases and the morphologies of ZnO nanostructures. A dye-sensitized solar cell assembled by the modified ZnO film electrode shows a power conversion efficiency of 1.66% for its ordered ZnO nanorod-arrays attached by ZnO nanoparticles for more dye absorption, direct electronic transportation and the reduction of charge recombination.

Keywords: ZnO nanorods; Electrodeposition; Dye-sensitized solar cells

1. Introduction

Demands for fossil fuels have been rapidly growing in company with the economic development in recent years. Excessive use of the fossil fuels has caused a serious of environmental problems which lead to the constraints of social progress and do harm to human health. Consequently great attention has been paid to the exploitation for new energy. Solar energy, a kind of green and abundant power source, is regarded as one of the most promising energetic resource for replacing the fossil fuels. It is well known that the employment of solar cells is an effective way to achieve the photoelectric conversion of solar energy. Compared to the conventional silicon-based solar cell, dye-sensitized solar cell (DSSC) is more attractive for its low-cost production, simple installment and wide flexibility since its prior appearance in 1991 [1,2]. Commonly, a DSSC is made up of a photoanode, electrolyte and a counter electrode. Much concern has been focused on the photoanode which is the pivotal component of DSSCs and plays a significant role for charge collection and transmission. Up to now, the best performances reported in the literature have been obtained with cells composed of a titania (TiO_2) nanoparticulate thin film sensitized by a ruthenium polypyridine complex dye (N3 and other derivatives) [3].

Besides TiO_2, zinc oxide (ZnO) is also investigated as another promising candidate for anode materials. The band gap energy and conduction band edge of ZnO are similar to those of TiO_2 [4,5]. Additionally, ZnO shows an order of magnitude higher electron mobility and the corresponding electron diffusion coefficient [6,7]. Recently, many studies have been focused on the quasi-one-dimensional (1D) nanostructured ZnO electrodes. Single crystal arrays have been the central research issues prominently such as nanorods [8,9], nanotubes [10] and nanowires [11], providing considerable direct path ways for timely electronic transportation and diminishing the chances of charge recombination [12]. By comparison, further improvement of efficiencies for DSSCs fabricated with ZnO nanoparticles films is restricted by the existence of numerous grain boundaries among nanoparticles, which is prone to the

*Corresponding author. Tel.: +86 59 26162225; fax: +86 592 6162225.
E-mail address: linyuyrr@163.com (Y. Lin).

0272-8842/$ - see front matter © 2013 Elsevier Ltd and Techna Group S.r.l. All rights reserved.
http://dx.doi.org/10.1016/j.ceramint.2013.07.065

occurrence of charge–hole recombination [13]. Therefore the 1D-ZnO arrays offer the possibilities to overcome the above defects and achieve the better DSSC properties undoubtedly.

However, the insufficient specific surface area of 1D nanomaterial has become the limitation for the performance promotion of 1D-ZnO-DSSC, which leads to the comparatively low efficiency owing to the poor dye loading and weak light trapping of 1D nanostructure [14]. One way to break the limit of 1D ZnO nanomaterials is to modify their surface status for the instance of branched nanorod arrays [15–17]. This manipulation would not only remain the advantages of 1D nanostructures for direct electronic transportation, but also enhance their surface area for more dye adsorption to form higher photocurrent.

The electrodeposited method is the most commonly used way for the preparation of ZnO nanoarrays. In the present work, a simple electrochemical deposition route is used at the first step to fabricate ZnO nanorod-arrays on the fluorine-doped tin oxide (FTO) glass substrates. After the nanorod-arrays being dipped into zinc acetate solution, the second deposited step is carried out in order to acquire the attachment and growth of ZnO nanoparticles around the nanorod-arrays. Simultaneously the effects on the morphologies of ZnO nanostructures with different electrodeposited parameters have been investigated and the photovoltaic performances of the DSSCs based on these ZnO nanostructured films have been measured.

2. Experimental section

2.1. Preparation of ZnO nanostructure thin films

The ZnO thin film was synthesized by a two step route of electrodeposition. All the reagents in the experiments were of analytical grade and no further purification was done. Firstly, ZnO nanorod arrays were grown by cathodic electrochemical deposition from an aqueous solution containing 5 mM to 50 mM of $Zn(NO_3)_2$. Zinc sheets (99.99% purity) and FTO glass substrates (pretreated by sonication in absolute ethanol and distilled water successively and dried in air at 40 °C) were used as the anode and cathode, respectively. The deposition temperature was fixed at 70 °C by a water bath. The deposited current was regulated at 0.5 mA. After 4 h of deposition, the ZnO nanorod arrays film was obtained and washed by deionized water several times. Then the as-prepared thin film was soaked into 50 ml alcoholic solution containing 0.25 g or 0.50 g $Zn(CH_3COO)_2$ for 2 h. Afterwards the thin film was taken out and annealed in a resistor furnace at 300 °C for 30 min. The second deposited procedure was performed by 2.5 mM $Zn(NO_3)_2$ solution from 1 h to 2 h with the same deposited current and temperature in the first step. After being rinsed by distilled water and annealed at 450 °C for 30 min, the final product was cooled at room temperature for further characterization.

2.2. Crystalline phase and morphological characterization

The phase composition and crystal structure of the as-electrodeposited ZnO nanostructures were identified by X-ray diffraction (XRD, Cu Kα radiation, SmartLab 3 kW, Rigaku, Japan) at a scanning rate of 4 deg min^{-1} in the range from 20° to 80°. The superficial morphologies of the ZnO thin films were observed by a field emission scanning electron microscope (SEM, Hitachi S-4800, Japan).

2.3. Cell fabrication and photoelectrochemical measurements

The FTO substrate deposited with ZnO thin layer was immersed into 0.25 mM anhydrous ethanol solution of indoline dye D149 and kept in dark place for 1 h. When loaded with dye molecules, the substrate with ZnO nanostructures was washed by ethanol, dried in the air naturally and performed as the photoanode. In addition, an electrodeposited platinum conductive glass was served as the counter electrode. Then the photoanode and the counter electrode were sandwiched together and the liquid electrolyte was dropped into the gap between the two electrodes by an injector in order to seep into the whole thin films. Ultimately a piece of cyano acrylate adhesive was applied as a sealant. The liquid electrolyte comprised of 0.6 M tetrabutyl ammonium iodide, 0.1 M lithium iodide, 0.1 M iodine and 0.5 M 4-tert-butylpyridine in a solution of acetonitrile. Herein, the cell assembly was completed. The photoelectrochemical properties of the above DSSCs were tested by measuring the current density–voltage (*J–V*) curves under simulated AM 1.5 solar illumination at 100 mW cm^{-2} intensity from a xenon arc lamp (XQ-500 W, Shanghai Photoelectricity Device Company, China) in ambient atmosphere and recording at an electrochemical workstation (CHI660C, Shanghai Chenhua Device Company, China).

3. Results and discussion

The XRD spectra of different samples obtained from each electrodeposited process are plotted in Fig. 1 so as to evaluate the crystal phases of ZnO nanostructures. All the typical

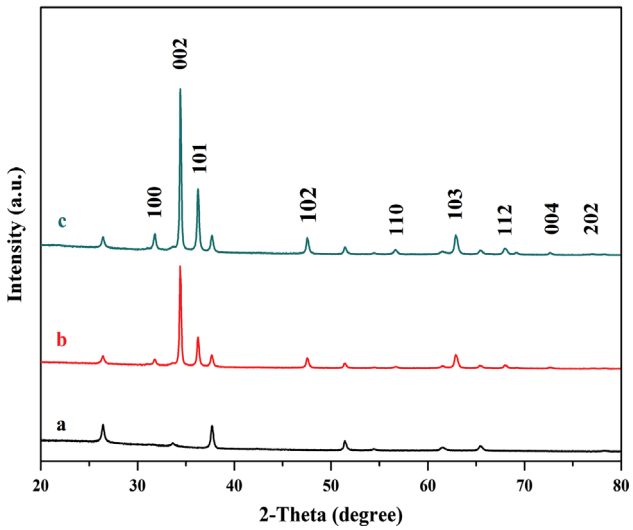

Fig. 1. XRD patterns of (a) the FTO substrate, (b) the first-step sample electrodeposited by 5 mM $Zn(NO_3)_2$ and (c) the sample after second-step deposition.

diffraction peaks can be well-indexed as the wurtzite ZnO phase in contrast with JCPDS card no. 36-1451, indicating that the products are of fine crystallization and no other impure phase is detected. From Fig. 1b, we can see that the sharpest peak appears at (002) orientation, which demonstrates that highly oriented ZnO nanorods along *c*-axis have been synthesized on the FTO substrates successfully via the electrodeposited approach in the liquid phase system. At the initial stage of the reaction, Zn^{2+} will move to the FTO-coated cathode directionally under the condition of an electric field, which induces the increasement of OH^- concentration and the formation of $Zn(OH)_2$ [18]. Then the conversion from $Zn(OH)_2$ to ZnO at 70 °C leads to the occurrence of numerous nucleation centers of ZnO which will attract more nucleation ions for aggregation. Because of the relatively low surface energy of (002) direction, its growth rate of ZnO crystal is faster compared to other directions and the ZnO nanorods are produced finally [19,20].

It is notable that the ZnO nanoparticles are generated by the decomposition of $Zn(CH_3COO)_2$ after soaking and annealing process and the chemical decomposed equation for $Zn(CH_3COO)_2$ at 300 °C can be described as the following reaction: $Zn(CH_3COO)_2+4O_2 \rightarrow ZnO+4CO_2+3H_2O$. These formed ZnO nanoparticles with high surface energy would attach to the primary structure of ZnO nanorod arrays and become the nucleation centers for the next step deposition [21]. After second step deposition, the intense (002) peak is reserved as shown in Fig. 1c, which can be ascribed to the well-crystallized ZnO nanorods of the secondary structure with small nanoparticles attaching or nanorods growing.

SEM photographs of the ZnO nanostructures prepared by different usage amounts of $Zn(CH_3COO)_2$ in soaking procedure and their *J–V* curves of DSSCs are displayed in Fig. 2. It is clearer that more ZnO nanoparticles have been loaded to the surface of ZnO nanorods when the ZnO nanorods film was soaked into the alcoholic solution of 0.50 g $Zn(CH_3COO)_2$ before the second-step electrodeposition. According to the

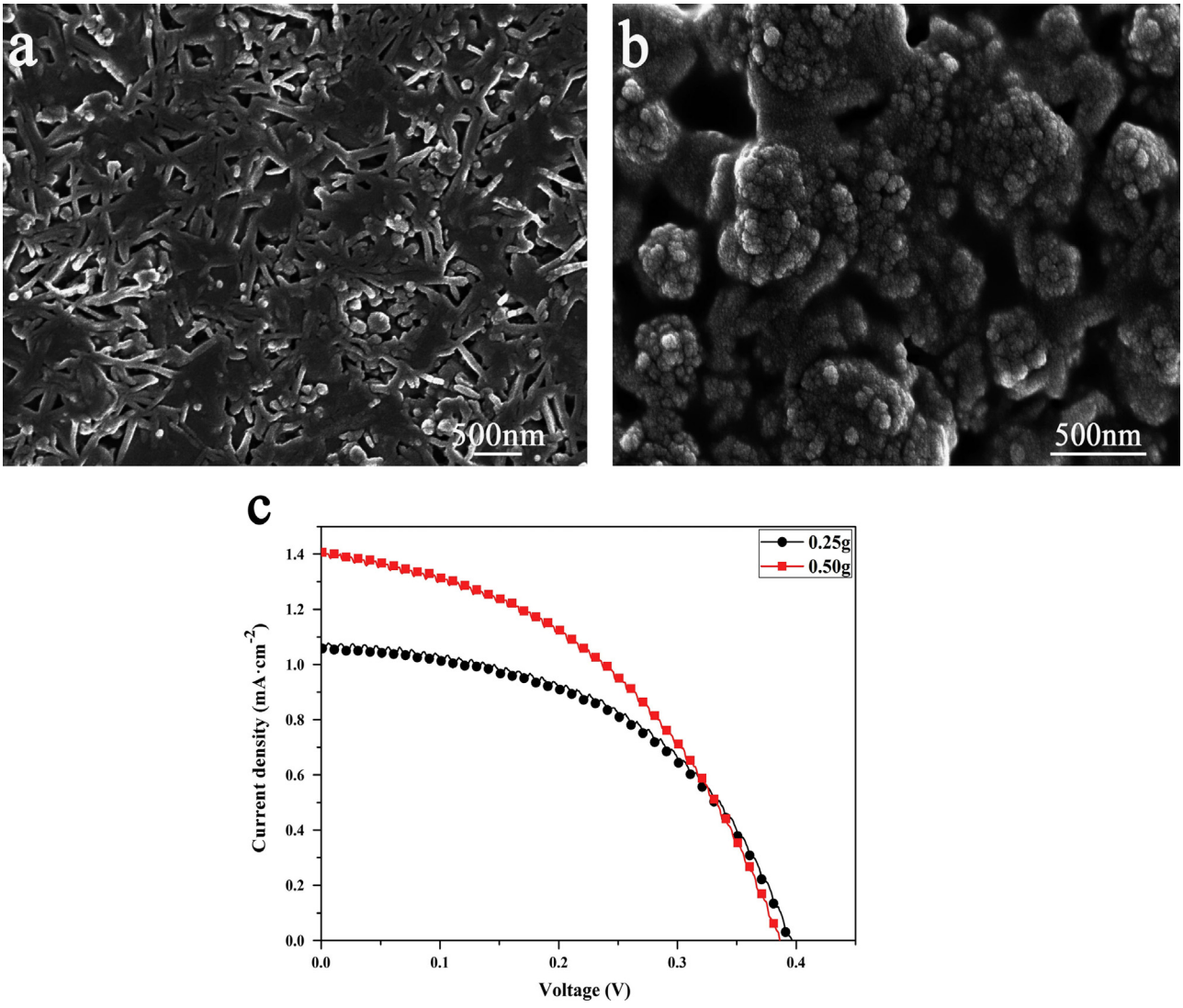

Fig. 2. SEM images of the ZnO synthesized by different dosages (a) 0.25 g, (b) 0.50 g of $Zn(CH_3COO)_2$ for soaking process and (c) their *J–V* curves of DSSCs. Prepared conditions for first-step deposition: 5 mM $Zn(NO_3)_2$, $t=4$ h, second-step deposition: 2.5 mM $Zn(NO_3)_2$, $t=2$ h.

photovoltaic performance data of DSSCs listed in Table 1, the sample of 0.50 g shows a higher short-circuit current density (J_{sc}) with 1.41 mA cm^{-2} and the photoelectric conversion efficiency (η) with 0.24% than the one of 0.25 g. This can be explained by that more usage of $Zn(CH_3COO)_2$ will produce more ZnO nanoparticles leading to more dye molecules absorbed and forming the better J_{sc} and η. To some degree, the higher open-circuit voltage (V_{oc}) for the sample of 0.25 g with 0.397 V is probably in line with the lower amount of its surface state.

Table 1
Performance data of DSSCs based on ZnO synthesized with different dosages of $Zn(CH_3COO)_2$ for the soaking process.

Sample (g)	V_{oc} (V)	J_{sc} (mA cm^{-2})	*FF*	η (%)
0.25	0.397	1.06	0.502	0.21
0.50	0.387	1.41	0.441	0.24

Table 2
Performance data of DSSCs based on ZnO synthesized with different deposited time for second-step deposition.

Sample (h)	V_{oc} (V)	J_{sc} (mA cm^{-2})	*FF*	η (%)
1	0.351	1.11	0.461	0.18
2	0.387	1.41	0.441	0.24

Fig. 3 presents the top views of the ZnO nanostructures produced with two different electrodeposited time for the second-step deposition and the *J–V* curves of DSSCs assembled by them. As we can see from these pictures, a considerable number of ZnO nanoparticles have been deposited onto the surface of rods. It is possible that the extension of the deposited time offers an opportunity for more ZnO nanoparticles to attach and crystallize around the primary structure of nanorods, which is able to absorb more dye molecules. And this is the reason why the sample of 2 h exhibits a better photocurrent with 1.41 mA cm^{-2} than 1 h as shown in Table 2. At the same time, the V_{oc} of 0.387 V for 2 h

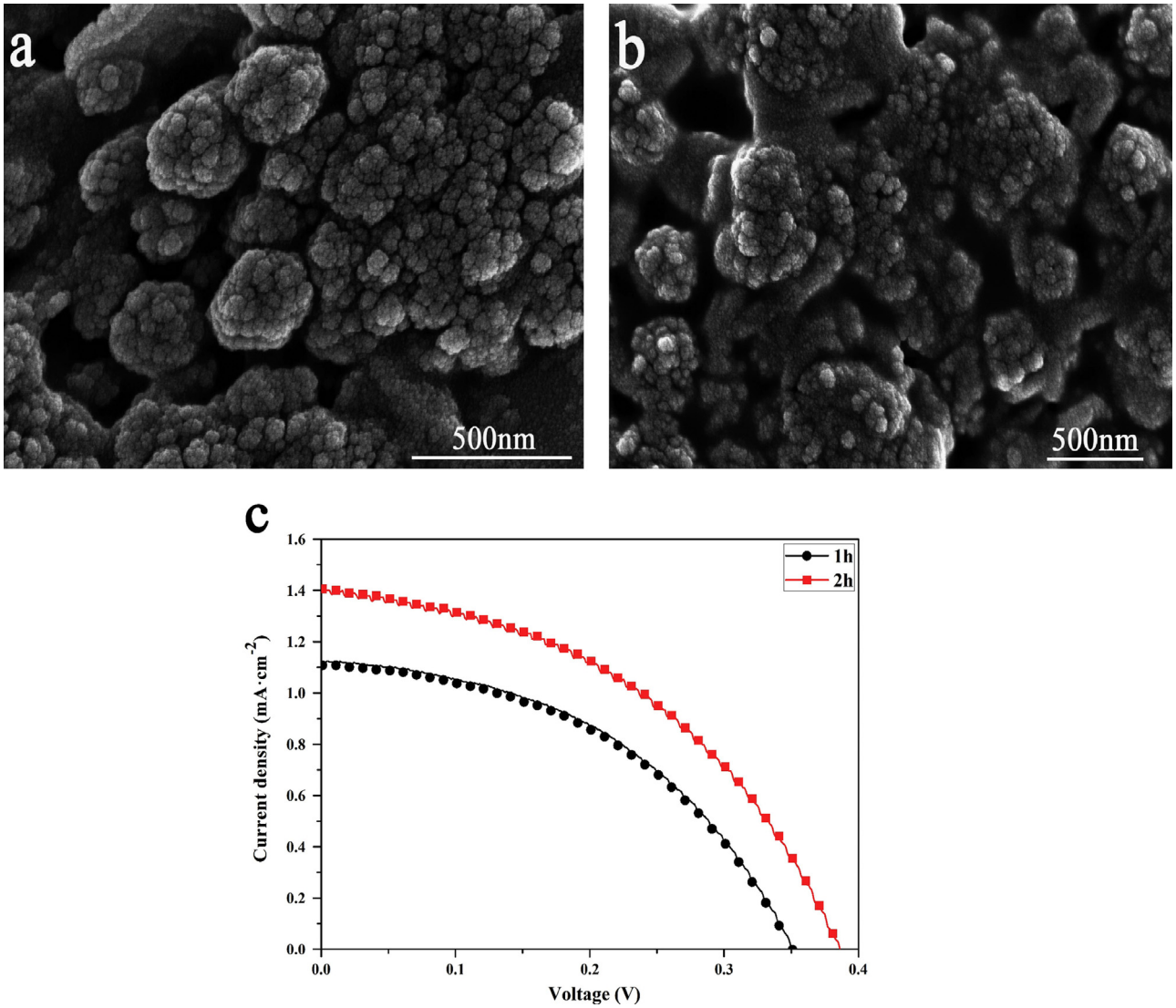

Fig. 3. SEM images of the ZnO synthesized with different deposited time (a) 1 h, (b) 2 h for second-step deposition and (c) their *J–V* curves of DSSCs. Prepared conditions for first-step deposition: 5 mM $Zn(NO_3)_2$, t=4 h, soaking process: 0.50 g $Zn(CH_3COO)_2$, second-step deposition: 2.5 mM $Zn(NO_3)_2$.

is higher than the one of 1 h, which may be related to the extent of the connection between the ZnO nanostructures within the thin film. Combining with the above factors, the better photoelectric property appears in the sample of 2 h.

SEM images of the ZnO nanostructures synthesized with various concentrations of $Zn(NO_3)_2$ solutions in the first-step deposited procedure and their *J–V* curves of DSSCs are exhibited in Fig. 4. In our previous work [22], it is found that the morphology of ZnO produced via one-step electrodeposition is the vast majority of ZnO nanorod arrays with a length about 4 μm when the concentration of $Zn(NO_3)_2$ is below 10 mM. However the ZnO product consisted of hexagonal columns is obtained at a higher $Zn(NO_3)_2$ concentration of 50 mM. These results have a great impact on the final morphologies of the ZnO films as seen in Fig. 4a–c. Based on the photovoltaic data of DSSCs summarized in Table 3, the sample of 10 mM shows the highest η of 1.66% with a remarkable J_{sc} of 5.97 mA cm^{-2}. The performance can be attributed to its structural advantages of the modification by nanoparticles around the single crystal ZnO nanorod-arrays after twice electrochemical deposition. These structures could not only be conducive for the direct electronic transmission and reduce the possibility of charge recombination, but also be able to furnish more surface area for more dye absorption than the bare ZnO nanorod-arrays because the uniform attachment of ZnO nanoparticles and the existence of the interspaces among these nanoparticles as seen in Fig. 4b are greatly helpful for the permeating of dye molecules to elevate the J_{sc}. By contrast, the other two samples are inferior in DSSC applications. This result is connected to the internal resistance of the cells and the density level of ZnO nanorods formed in the first-step deposition, which is determined that whether there is enough space for the permeating of $Zn(CH_3COO)_2$

Table 3
Performance data of DSSCs based on ZnO synthesized with different Zn $(NO_3)_2$ concentrations for 4 h in the first-step deposition.

Sample (mM)	V_{oc} (V)	J_{sc} (mA cm^{-2})	*FF*	η (%)
5	0.387	1.41	0.441	0.24
10	0.569	5.97	0.489	1.66
50	0.572	2.42	0.444	0.61

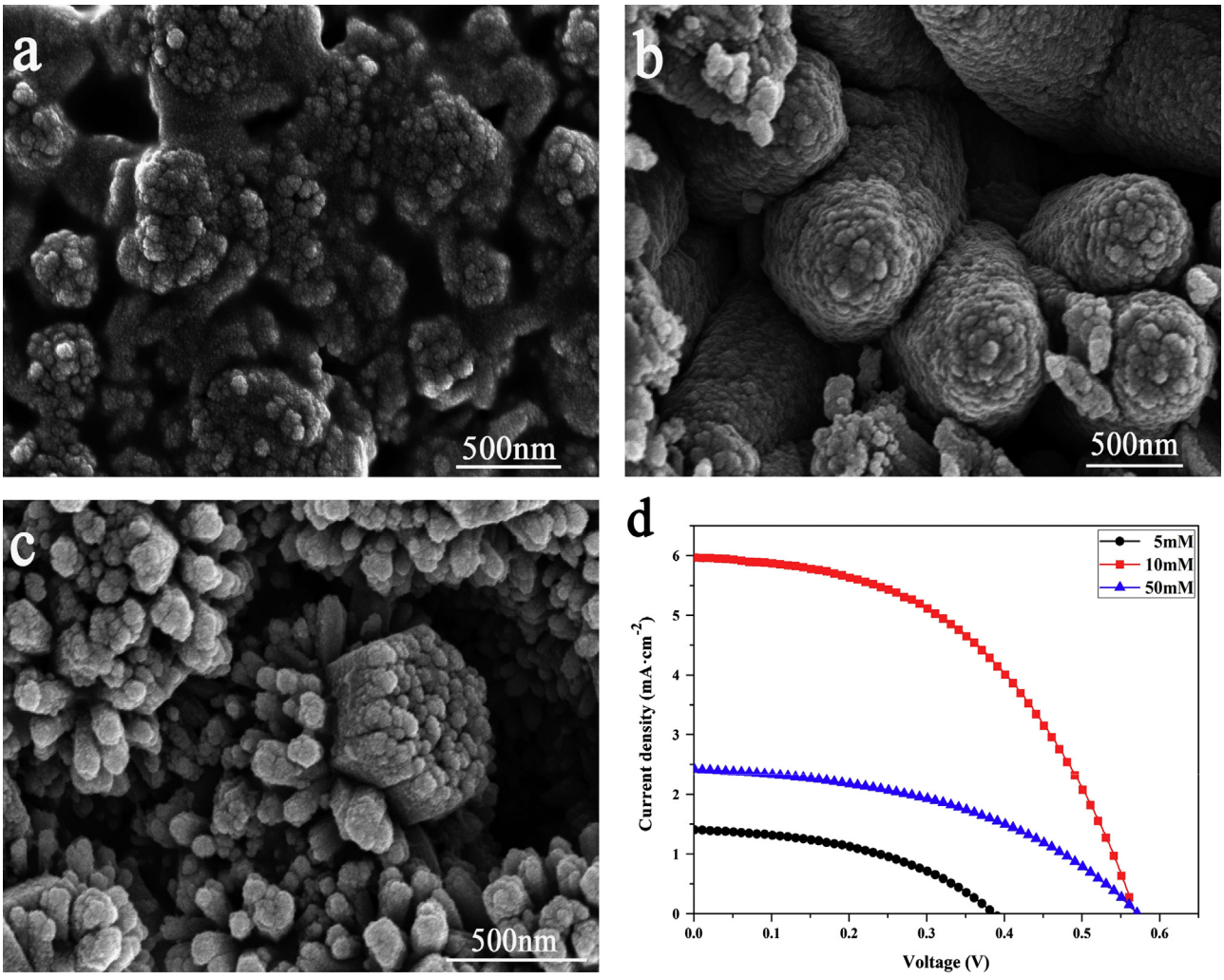

Fig. 4. SEM images of the ZnO synthesized with different concentrations (a) 5 mM, (b) 10 mM, (c) 50 mM of $Zn(NO_3)_2$ for 4 h in first-step deposition and (d) their *J–V* curves of DSSCs. Prepared conditions for the soaking process: 0.50 g $Zn(CH_3COO)_2$, second-step deposition: 2.5 mM $Zn(NO_3)_2$, $t=2$ h.

solution in the soaking process and the growth of ZnO nanoparticles in the second-step deposition.

4. Conclusions

In summary, a two step electrochemical deposited route is employed to modify the surface state of 1D-ZnO nanorods. The influences of electrodeposited parameters on the morphologies and performances of the DSSCs have been studied in this work. The sample after deposition of 10 mM $Zn(NO_3)_2$ solution for 4 h in first step, soaking in 0.50 g $Zn(CH_3COO)_2$ ethanol solution and second-deposition of 2.5 mM $Zn(NO_3)_2$ solution for 2 h presents the best energy conversion efficiency of 1.66% with a short-circuit photocurrent density of 5.97 mA cm^{-2} owing to the structural superiority for its ordered ZnO nanorods modified by ZnO nanoparticles, which offers an approach for the photovoltaic enhancement of 1D-ZnO-DSSCs.

Acknowledgment

This work was supported by the Fundamental Research Funds for the Central Universities (Grant no. JB-ZR1137).

References

[1] B. O′Regan, M. Grätzel, A low-cost, high-efficiency solar cell based on dye-sensitized colloidal TiO_2 films, Nature 353 (1991) 737–740.
[2] M. Grätzel, Photoelectrochemical cells, Nature 414 (2001) 338–344.
[3] A. Yella, H.W. Lee, H.N. Tsao, C.Y. Yi, A.K. Chandiran, M. K. Nazeeruddin, E.W.G. Diau, C.Y. Yeh, S.M. Zakeeruddin, M. Grätzel, Porphyrin-sensitized solar cells with cobalt(II/III)-based redox electrolyte exceed 12 percent efficiency, Science 334 (2011) 629–634.
[4] P. Tiwana, P. Docampo, M.B. Johnston, H.J. Snaith, L.M. Herz, Electron mobility and injection dynamics in mesoporous ZnO, SnO_2, and TiO_2 films used in dye-sensitized solar cells, ACS Nano 5 (2011) 5158–5166.
[5] J. Gong, J. Liang, K. Sumathy, Review on dye-sensitized solar cells (DSSCs): fundamental concepts and novel materials, Renewable and Sustainable Energy Reviews 16 (2012) 5848–5860.
[6] M. Quintana, T. Edvinsson, A. Hagfeldt, G. Boschloo, Comparison of dye-sensitized ZnO and TiO_2 solar cells: studies of charge transport and carrier lifetime, Journal of Physical Chemistry C 111 (2007) 1035–1041.
[7] I.G. Valls, M.L. Cantu, Vertically-aligned nanostructures of ZnO for excitonic solar cells: a review, Energy and Environmental Science 2 (2009) 19–34.
[8] Y. Xie, P. Joshi, S.B. Darling, Q.L. Chen, T. Zhang, D. Galipeau, Q. Q. Qiao, Electrolyte effects on electron transport and recombination at ZnO nanorods for dye-sensitized solar cells, Journal of Physical Chemistry C 114 (2010) 17880–17888.
[9] J.Y. Chung, J.Y. Lee, S.W. Lim, Annealing effects of ZnO nanorods on dye-sensitized solar cell efficiency, Physica B 405 (2010) 2593–2598.
[10] J.Y. Yang, Y. Lin, Y.M. Meng, Y.H. Liu, A two-step route to synthesize highly oriented ZnO nanotube arrays, Ceramics International 38 (2012) 4555–4559.
[11] G.Y. Chen, K.B. Zheng, X.L. Mo, D.L. Sun, Q.H. Meng, G.R. Chen, Metal-free indoline dye sensitized zinc oxide nanowires solar cell, Materials Letters 64 (2010) 1336–1339.
[12] L. Li, T.Y. Zhai, Y. Bando, D. Golberg, Recent progress of one-dimensional ZnO nanostructured solar cells, Nano Energy 1 (2012) 91–106.
[13] Q.F. Zhang, G.Z. Cao, Nanostructured photoelectrodes for dye-sensitized solar cells, Nano Today 6 (2011) 91–109.
[14] J.A. Anta, E. Guillén, R.T. Zaera, ZnO-based dye-sensitized solar cells, Journal of Physical Chemistry C 116 (2012) 11413–11425.
[15] W. Chen, Y.C. Qiu, S.H. Yang, Branched ZnO nanostructures as building blocks of photoelectrodes for efficient solar energy conversion, Physical Chemistry Chemical Physics 14 (2012) 10872–10881.
[16] C.T. Wu, W.P. Liao, J.J. Wu, Three-dimensional ZnO nanodendrite/nanoparticle composite solar cells, Journal of Materials Chemistry 21 (2011) 2871–2876.
[17] S.H. Ko, D. Lee, H.W. Kang, K.H. Nam, J.Y. Yeo, S.J. Hong, C. P. Grigoropoulos, H.J. Sung, Nanoforest of hydrothermally grown hierarchical ZnO nanowires for a high efficiency dye-sensitized solar cell, Nano Letters 11 (2011) 666–671.
[18] S. Peulon, D. Lincot, Cathodic electrodeposition from aqueous solution of dense or open-structured zinc oxide films, Advanced Materials 8 (1996) 166–170.
[19] L. Vayssieres, K. Keis, S.E. Lindquist, A. Hagfeldt, Purpose-built anisotropic metal oxide material: 3D highly oriented microrod array of ZnO, Journal of Physical Chemistry B 105 (2001) 3350–3352.
[20] M. Guo, C.Y. Yang, M. Zhang, Y.J. Zhang, T. Ma, X.D. Wang, X. D. Wang, Effects of preparing conditions on the electrodeposition of well-aligned ZnO nanorod arrays, Electrochimica Acta 53 (2008) 4633–4641.
[21] J.H. Qiu, M. Guo, Y.J. Feng, X.D. Wang, Electrochemical deposition of branched hierarchical ZnO nanowire arrays and its photoelectrochemical properties, Electrochimica Acta 56 (2011) 5776–5782.
[22] Y. Lin, J.Y. Yang, X.Y. Zhou, Controlled synthesis of oriented ZnO nanorod arrays by seed-layer-free electrochemical deposition, Applied Surface Science 258 (2011) 1491–1494.